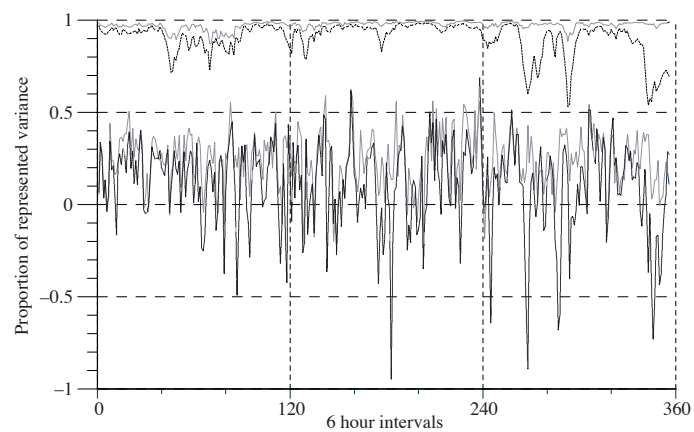


## Long-wave forcing for regional atmospheric modelling



**Authors:**

**H. von Storch**

**H. Langenberg**

**F.Feser**

(Institute of Hydrophysics)

## Long-wave forcing for regional atmospheric modelling

H. von Storch, H. Langenberg, F. Feser

*32 pages with 12 figures and 2 tables*

### Abstract

A new method, named "spectral nudging", of linking a regional model to the driving large-scale model simulated or analyzed by a global model is proposed and tested. Spectral nudging is based on the idea that regional-scale climate statistics are conditioned by the interplay between continental-scale atmospheric conditions and such regional features as marginal seas and mountain ranges. Following this "downscaling" idea, the regional model is forced to satisfy not only boundary conditions, possibly in a boundary sponge region, but also large-scale flow conditions inside the integration area.

We demonstrate that spectral nudging succeeds in keeping the simulated state close to the driving state at larger scales, while generating smaller-scale features. We also show that the standard boundary forcing technique in current use allows the regional model to develop internal states conflicting with the large-scale state. It is concluded that spectral nudging may be seen as a suboptimal and indirect data assimilation technique.

## Langweilliger Antrieb für regionale atmosphärische Modellierung

### Zusammenfassung

Eine neue Methode, genannt "spektrales nudging", ein Regionalmodell an das durch ein Globalmodell simulierte großskalige Antriebsfeld zu koppeln, wird vorgestellt und getestet. Das spektrale nudging basiert auf der Annahme, daß regionale Klimastatistik durch die Wechselwirkung zwischen dem kontinental-skaligen atmosphärischen Zustand und regionalen Gegebenheiten, wie kleinere Seen und Gebirgszüge, bestimmt wird. Demnach muß das Regionalmodell nicht nur die Randbedingungen erfüllen, sondern auch die großskaligen Zustände innerhalb des Integrationsgebietes wiedergeben können.

Wir zeigen, daß durch das spektrale nudging der großskalige modellierte Zustand nahe an dem des Antriebsfeldes liegt, ohne die Modellierung regionaler Phänomene zu beeinträchtigen. Außerdem zeigen wir, daß das Regionalmodell durch die zur Zeit benutzte Antriebstechnik über den Modellrand interne Felder produzieren kann, die zu dem großskaligen Zustand im Widerspruch stehen. Wir schließen daraus, daß das spektrale nudging als eine suboptimale, indirekte Datenassimilierungsmethode angesehen werden kann.

# Contents

<b>1</b>	<b>Background</b>	<b>7</b>
<b>2</b>	<b>REMO model</b>	<b>9</b>
<b>3</b>	<b>Spectral Nudging</b>	<b>11</b>
<b>4</b>	<b>Results</b>	<b>13</b>
4.1	Efficiency of Large-Scale Control . . . . .	13
4.2	Comparison with observational data . . . . .	22
4.3	Sensitivity experiments . . . . .	26
<b>5</b>	<b>Conclusions</b>	<b>26</b>
<b>6</b>	<b>Acknowledgments</b>	<b>27</b>
<b>7</b>	<b>References</b>	<b>28</b>



# 1 Background

The state of the atmosphere can not be observed in its entirety. Only samples of mostly point observations irregularly distributed in space are available. They are used by operational weather centers to construct, or “analyze”, a continuous distribution of atmospheric variables. Such “analyses” are our best guess of the atmospheric state and deviate from the true, unknown state to some extent. Likely, the large scales are best described, simply because they are better sampled. On the other hand, the details on scales of a few tens of kilometers and less, are insufficiently sampled and subject to significant uncertainty.

In old days, the analyses were prepared by hand, and a major achievement of meteorology was the finding by the Bergen school at about 1920 that the appearance of the sky contains information about the state of the atmosphere which should be incorporated into the analysis and weather forecasting process (Friedmann, 1989). The advent of satellites, with their quasi-complete mapping of horizontal distributions, has improved the situation considerably. The major breakthrough was the systematic interpretation of observational data aided by quasi-realistic dynamical models. However, the only features which can be well reproduced by these objective analyses with quasi-realistic models are those that are well resolved by the model. For example, while the effect of the Baltic Sea may to some extent be captured, the imprint of Jutland, separating the Baltic Sea from the North Sea, may not. Thus, the lacking detail in analyses remains at present a major problem in weather analyses.

While in former days the purpose of weather, or synoptic, analyses was for preparing short-term weather forecasts, these analyses have in recent years attained a different role, namely to provide a data base for climatic and other environmental studies. For fulfilling this purpose, it is no longer sufficient to have the best analysis at a given day. It is also necessary that the quality of the analyses is homogeneous, so that improvements of the analysis process do not introduce artificial signals in the climate data set. For meeting this requirements, weather services have prepared so-called global re-analyses, i.e., they have analyzed weather observations of the past decades with the same analysis scheme (Kalnay et al., 1996).

We suggest a new technique for using these global re-analyses to derive smaller-scale analyses.

Our technique is based on the view that small scale details are the result of an interplay between larger-scale atmospheric flow and smaller-scale geographic features such as topography, land-sea distribution or land-use (von Storch, 1999). To describe this small-scale response, a regional climate model is forced with large-scale weather analyses. Differently from the conventional approach, the forcing is not only stipulated at the lateral boundaries but also in the interior. This interior forcing is maintained by adding nudging terms in the spectral domain, with maximum efficiency for large scales and no effect for small scales. We name the technique “spectral nudging”. Also, the efficiency is formulated to depend on height and the variable under consideration. As far as we know this technique is new, but it shares similarities with methods to force area averages upon the interior solution as proposed by Kida et al. (1991) and Sasaki et al. (1995). Our method makes use of Giorgi et al.’s (1993) approach who introduce a height-dependent forcing of their regional model.

For purposes of weather analysis, our proposed technique is suboptimal. Ideally, inside the model area one would directly assimilate local observational data, which had little impact on the coarse-grid global re-analyses and, accordingly, were not fully exploited. However, such a scheme is technically very demanding and often not feasible. The proposed technique may be considered a “poor woman’s data assimilation technique”.

The same technique may be used to derive regional scale climate change scenarios from global climate models (“downscaling”; von Storch, 1995). The basic idea of downscaling is to transfer onto smaller scales that large-scale information which has been simulated reliably in climate change scenarios. This is done with the help of statistical models or dynamical regional climate models. The latter technique, named “dynamical downscaling” uses output from global climate models to force regional atmospheric (e.g., Giorgi (1990), Jacob and Podzun (1997), Kidson and Thompson (1998), Rinke and Dethloff (1999)) or regional oceanic model (Kauker, 1999). In nearly all studies performed to date, the forcing is administered exclusively at the lateral boundaries. The technique of statistical dynamical downscaling developed by Fuentes and Heimann (1996) and Frey-Buness et al. (1995) is related to our approach, as they consider the response of a regional climate model to prescribed conditions such as the geostrophic wind.

In our view, the conventional practise of using forcing exclusively along the lateral boundaries

stems from the classic view of regional weather modeling as being a boundary problem rather than a downscaling problem. Problems like data assimilation and downscaling were not considered in classical numerical mathematics. The inclusion of the “sponge zone” (Davies, 1976) was already a violation of the “pure” mathematical concept. In this paper we demonstrate that the boundary value format is conceptually inappropriate for the problem at hand.

The present paper is organized as follows. A brief introduction of the regional atmospheric model is given in Section 2. The spectral nudging technique is described in Section 3, and the results are presented and discussed in Section 4. The discussion makes use of measures, which quantify the degree of similarity or dissimilarity on different spatial scales. Sensitivity experiments dealing with the strength of the coupling are considered. Conclusions are summarized in Section 5.

## 2 REMO model

We use the regional climate model REMO as described by Jacob and Podzun (1997). REMO is a grid point model featuring the discretized primitive equations in a terrain-following hybrid coordinates system. Details are given by Jacob and Podzun (1997) and Jacob et al. (1995). The finite differencing scheme is energy preserving. The prognostic variables are surface pressure, horizontal wind components, temperature, specific humidity and cloud water. A soil model is added to account for soil temperature and water content.

The integration area shown in Figure 1 has a horizontal spherical resolution of  $0.5^\circ$  with a pole at  $170^\circ W, 35^\circ N$ , resulting in  $91 \times 81$  grid points. Because of the spherical resolution, the straight grid lines shown in the map are only approximate. A time step of 5 minutes is adopted.

REMO is forced with NCEP re-analyses (Kalnay et al., 1996) over the three month period of January to March 1993. These observed states are updated every six hours. In between, values are derived through linear interpolation. The horizontal resolution of the analyses is approximately  $2^\circ$  longitudinally and latitudinally (Figure 2). Since REMO operates with a



Figure 1: The model area and the REMO grid. Solid lines demarcate 100 ( $10 \times 10$ ) grid boxes. Because of the spherical resolution, the straight lines are only approximations.

rotated spherical grid, its coverage with NCEP grid-boxes is inhomogeneous. In the north-south direction, there are 21 NCEP boxes, and in the east-west direction, 27 boxes along the southern margin and 48 along the northern margin. That is, the REMO model offers a resolution enhanced by factor of 1:16, on average. Maximum improvement of resolution is achieved in the southern part of the integration area.

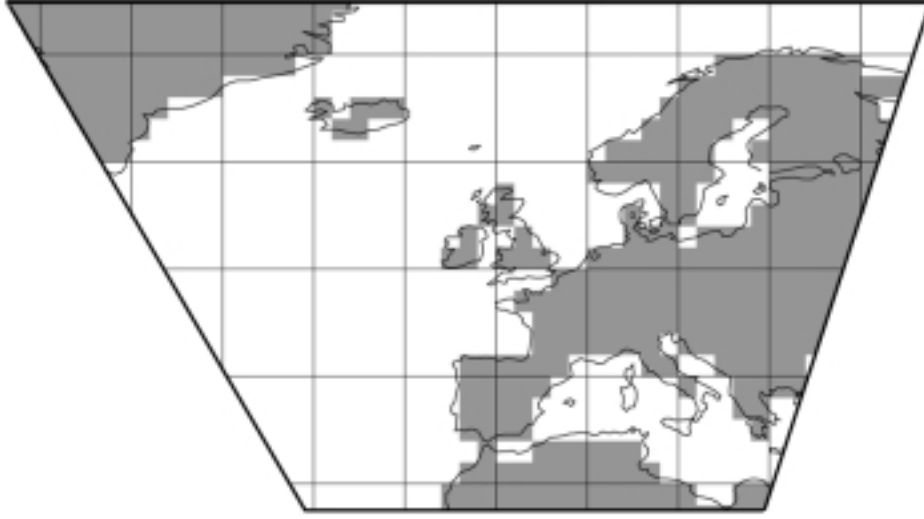


Figure 2: The REMO model domain and the NCEP grid. The lines demarcate every fifth grid box.

### 3 Spectral Nudging

As outlined in the Introduction, we have used two different approaches to force the regional model to follow the steering provided by the analyses. In the “standard” approach in current use, the steering takes place exclusively along the lateral boundaries in the spirit of a classical boundary value problem. In the “spectral nudging” approach, the atmospheric state inside the integration area is also forced to accept the analyses for large-scales whereas smaller scales are left to be determined by the regional model.

In the standard setup, the observed state is forced upon the model in a lateral boundary zone covering 8 grid points using Davies’ (1976) classical “sponge” technique: The “interior” solution of the model, denoted  $\Psi$ , is brought closer to, or “nudged” to the observed state, denoted  $\Psi^*$ , by adding an adjustment or restoring term  $\gamma \cdot (\Psi^* - \Psi)$ , where the “nudging coefficient”  $\gamma$  takes largest values at the lateral boundary and decreases towards the interior of the integration domain. When  $\Psi > \Psi^*$ , the restoring terms causes a decrease in  $\Psi$ , and when  $\Psi < \Psi^*$  an increasing tendency of  $\Psi$  is induced. The nudging coefficient has units of 1/time. This standard approach is commonly used in regional weather forecasting and regional

climate simulations. The “sponge” zone has been introduced to avoid reflection of traveling features at the boundaries. Any inconsistencies stemming from internally generated features traveling towards the lateral boundaries and conflicting there with the prescribed conditions are dampened out in this manner.

In the “spectral nudging” approach, the lateral “sponge forcing” is kept and an additional steering is introduced as described next.

Consider the expansion of a suitable REMO variable:

$$\Psi(\lambda, \phi, t) = \sum_{j=-J_m, k=-K_m}^{J_m, K_m} \alpha_{j,k}^m(t) e^{ij\lambda/L_\lambda} e^{ik\phi/L_\phi} \quad (1)$$

with zonal coordinates  $\lambda$ , zonal wave-numbers  $j$  and zonal extension of the area  $L_\lambda$ . Meridional coordinates are denoted by  $\phi$ , meridional wave-numbers by  $k$ , and the meridional extension by  $L_\phi$ .  $t$  represents time. For REMO, the number of zonal and meridional wave-numbers is  $J_m$  and  $K_m$ . A similar expansion is done for the analyses, which are given on a coarser grid. The coefficients of this expansion are labeled  $\alpha_{j,k}^a$ , and the number of Fourier coefficients is  $J_a < J_m$  and  $K_a < K_m$ . The confidence we have in the realism of the different scales of the re-analysis depends on the wavenumbers  $j$  and  $k$  and is denoted by  $\eta_{j,k}$ .

The model is then allowed to deviate from the state given by the re-analysis conditional upon this confidence. This is achieved by adding “nudging terms” in the spectral domain in both directions

$$\sum_{j=-J_a, k=-K_a}^{J_a, K_a} \eta_{j,k} (\alpha_{j,k}^a(t) - \alpha_{j,k}^m(t)) e^{ij\lambda/L_\lambda} e^{ik\phi/L_\phi} \quad (2)$$

In the following, we will use the nudging terms dependent on height. That is, our confidence in the reanalyses increases with height. On the other hand, we leave the regional model more room for its own dynamics at the lower levels where we expect regional geographical features are becoming more important. The better the confidence, the larger the  $\eta_{j,k}$ -values and the more efficient the nudging term.

In this study, we have applied nudging to the zonal and meridional wind components. Following the prescription of the German Weather Service version of REMO, which uses a pointwise nudging in case of excessively high wind speeds for preventing numerical instability, we have

adopted the vertical profile

$$\eta^0(p) = \begin{cases} \alpha \left(1 - \frac{p}{850hPa}\right)^2 & \text{for } p < 850hPa \\ 0 & \text{for } p > 850hPa \end{cases} \quad (3)$$

with  $p$  denoting pressure (Doms et al., 1995). In our base simulation with spectral nudging we used the ad-hoc value  $\alpha = 0.05$ , resulting in a vertical profile as shown in Figure 3. This choice amounts to an e-folding decay time of an introduced disturbance of about 60 days at 850 hPa, 1 day at 500 hPa and about 3 hours at the model’s top level of 25 hPa.

We have set  $\eta_{j,k} = \eta^0$  for  $j = 0 \dots 3$  in the north-south direction,  $k = 0 \dots 5$  in the east-west direction and  $\eta_{j,k} = 0$  otherwise. That is, wavelengths of about  $15^\circ$  and larger are considered to be reliably analysed by NCEP, corresponding to 6 and more NCEP grid points. More elaborate specifications could certainly have been used. However, some sensitivity experiments indicated that the effect would be somewhat marginal (see below).

## 4 Results

We demonstrate in Section 4.1 that spectral nudging successfully prevents the regional model from deviating from the given large-scale state. We also show that significant deviations take place when the standard approach is used. In Section 4.2, a comparison with station data reveals that the spectral control is limited to the largest scales, so that the representation of the local time series is indeed improved compared to the NCEP reanalysis and the REMO standard run. In Section 4.3, a number of sensitivity experiments is presented and discussed.

### 4.1 Efficiency of Large-Scale Control

We divide the spectral domain into several intervals. We assume that both the regional and global model have two spectral domains: a large-scale domain,  $\mathcal{L}$  and a small-scale domain,  $\mathcal{S}$ . The model has different skills in the domains  $\mathcal{L}$  and  $\mathcal{S}$  to realistically analyze or simulate the real state. Only the results in  $\mathcal{L}$  are considered reliable. So far there is no objective way to identify the interval  $\mathcal{L}$ , but it is often believed that the largest wave-number in  $\mathcal{L}$  is several

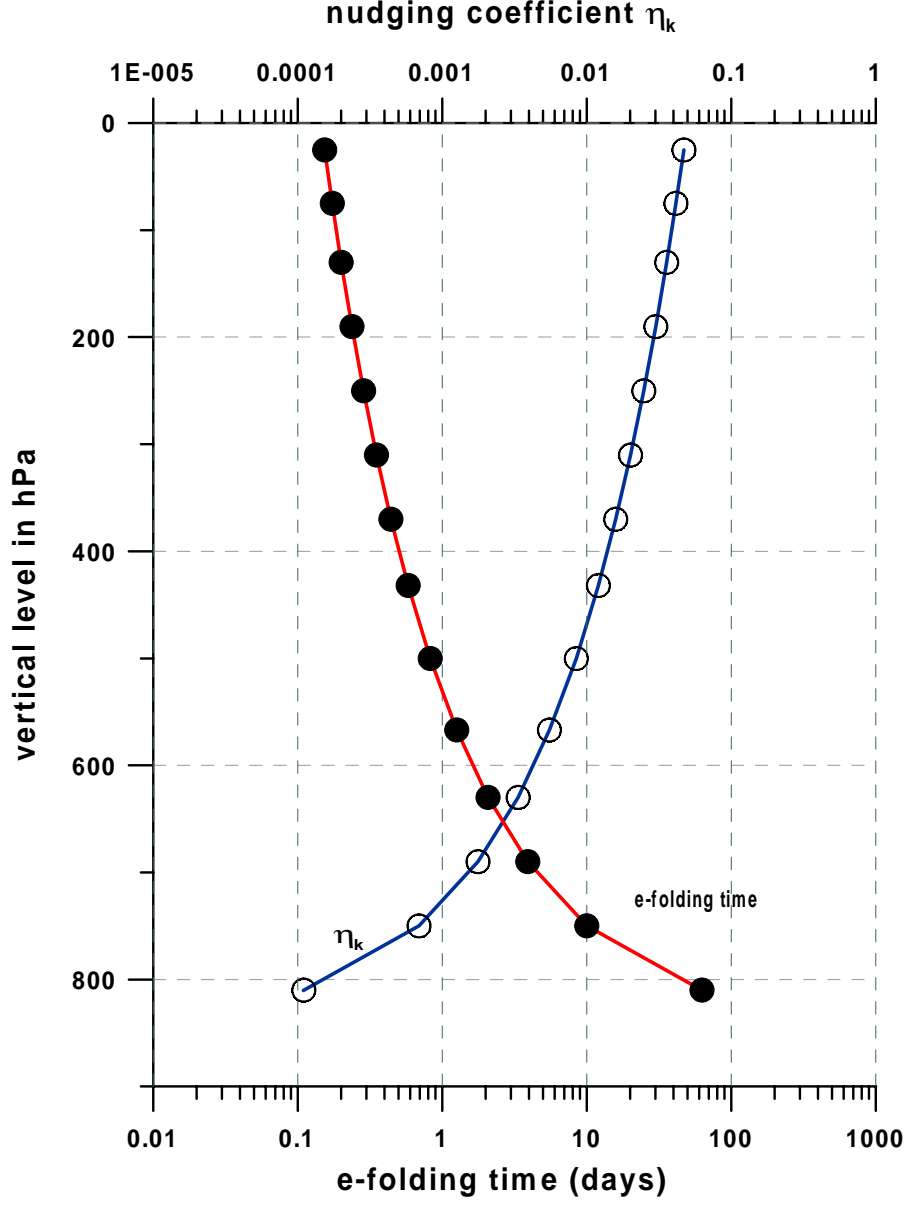


Figure 3: Vertical distribution of the spectral nudging term  $\eta^0$  (open circles) and corresponding e-folding time in days (closed circles).

mesh-sizes of the model's grid. Since the global model and the regional model have different grids, their “reliable” domains,  $\mathcal{L}_g$  and  $\mathcal{L}_r$ , are different (Figure 4). In  $\mathcal{L}_g \cap \mathcal{L}_r$  the results of the regional model should not deviate from the global analyses, as the results of  $\mathcal{L}_g$  are considered skillful. Therefore, for these scales, large values of  $\eta_k$  are adopted. However, in the domain

$\mathcal{S}_g \cap \mathcal{L}_r$  significant modifications are expected and wanted, because the regional model has the role of adding detail in these spatial scales. Accordingly, the nudging term  $\eta_k$  is set to zero for these scales.

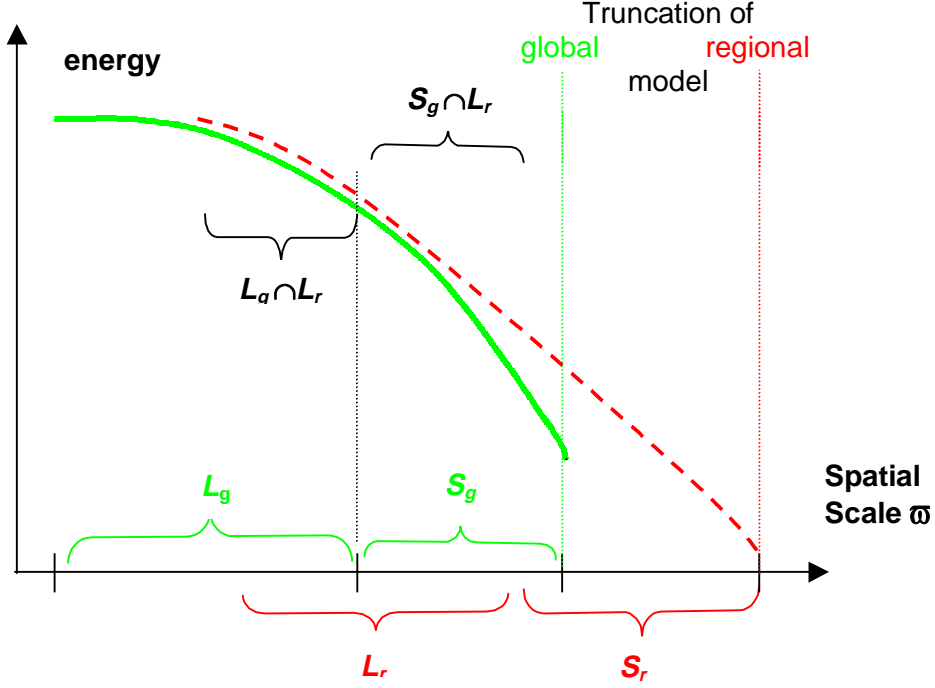


Figure 4: Sketch of spatial ranges  $\mathcal{L}$  and  $\mathcal{S}$  of global analyses and regional model.

We measure the similarity of input NCEP fields and output REMO fields at time  $t$  by the proportion of spatial variability of the output described by the input:

$$\mathcal{P}(t) = 1 - \frac{\langle (\Psi(t) - \Psi^*(t))^2 \rangle}{\langle \Psi(t)^2 \rangle} \quad (4)$$

where  $\Psi(t)$  is the output REMO field at time  $t$ ,  $\Psi^*$  the input NCEP field, and  $\langle \cdot \rangle$  a spatial average. When this averaging is done for scales  $\omega \in \mathcal{L}_g \cap \mathcal{L}_r$ , we denote the similarity measure as  $\mathcal{P}_g$ . This number should be close to one, as we do not want to modify the scales reliably described by the NCEP analysis. However, for the spectral domain  $\mathcal{S}_g \cap \mathcal{L}_r$ , we do not request the REMO field to be similar to the input fields, so that the measure of similarity  $\mathcal{P}_r$  may be much smaller than 1.

In the present analysis, the set  $\mathcal{L}_g \cap \mathcal{L}_r$  is set to comprise zonal wavenumbers up to  $k \leq 5$  and meridional wavenumbers  $j \leq 3$ , so that for all  $(j, k) \in \mathcal{L}_g \cap \mathcal{L}_r$   $\eta_{j,k} = \eta^0$ . The domain  $\mathcal{S}_g \cap \mathcal{L}_r$  contains  $5 < k \leq 13$  and  $3 < j \leq 10$  so that  $\eta_{j,k}$  is zero for these scales. Note that the exact definition of these sets is inconsequential for the performance of the nudging technique as the numbers  $\mathcal{P}_g$  and  $\mathcal{P}_r$  are diagnostics; in fact also the diagnostic results are rather insensitive to the details of this choice.

The time series of the similarity measures,  $\mathcal{P}_g$  and  $\mathcal{P}_r$ , calculated for both the standard run and for the spectral nudging run, have been calculated for relative humidity and temperature as well as for the zonal and meridional wind components at 850 and 500 hPa. For the sake of brevity results are shown only for the meridional wind at 500 hPa in Figure 5.

The desired effect of a greater similarity in the spectral range  $\mathcal{L}_g \cap \mathcal{L}_r$  is achieved in the spectral nudging run. In terms of temperature and humidity  $\mathcal{P}_g$  hardly deviates from the ideal value of 1 in the spectral nudging run (not shown), whereas in the boundary forcing run for the meridional wind component values less than 1, sometimes as low as 0.6 are obtained (Figure 5).  $\mathcal{P}_r$  values between 20% and 40% indicate that REMO considerably modifies the scales that had been insufficiently resolved by NCEP.  $\mathcal{P}_r$  is mostly somewhat smaller for the standard boundary forcing run, i.e., controlling the large-scale features in  $\mathcal{L}_g$  has some effect on  $\mathcal{S}_g \cap \mathcal{L}_r$  as well. However, the variances in  $\mathcal{S}_g \cap \mathcal{L}_r$  are similar in both runs, with forcing limited to the boundary and spectral nudging. This is exemplified by table 1 listing averaged variances for the different spatial scales for the zonal and meridional wind components at 850 hPa.

The variance in the large-scale domain of the NCEP analyses ( $\mathcal{L}_g$ ) is about reproduced by both REMO runs, while the variances in the spatial domain well resolved by REMO but less well by NCEP ( $\mathcal{S}_g \cap \mathcal{L}_r$ ) is markedly larger in both regional models than in the global analyses. In fact, the simulation with nudging is attaining even larger variances than the standard run.

As the nudging is applied to velocity only, the effect is strongest in these variables, whereas the difference is significant but somewhat less dramatic in terms of temperature or humidity (not shown).

With the standard boundary forcing, episodes emerge with patterns quite dissimilar to the

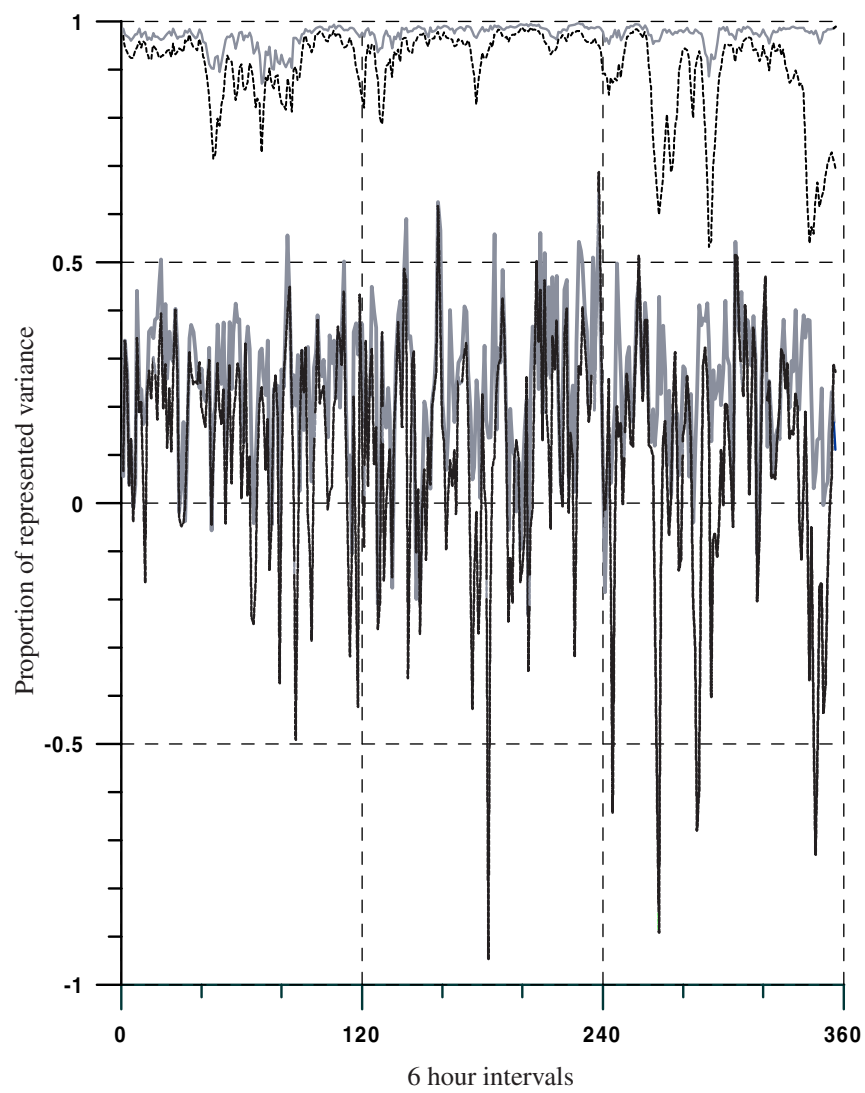
Table 1:

scale/variable	units	NCEP	REMO	REMO
	$m^2 s^{-2}$	analyses	standard	nudging
zonal wind				
$\mathcal{L}_g$	$10^{-2}$	1.6	1.2	1.6
$\mathcal{S}_g \cap \mathcal{L}_r$	$10^{-6}$	3.7	7.7	8.1
meridional wind				
$\mathcal{L}_g$	$10^{-2}$	1.4	1.3	1.5
$\mathcal{S}_g \cap \mathcal{L}_r$	$10^{-6}$	2.1	6.5	8.5

driving NCEP analysis. An example is the episode of 9-12 March, which is marked by low  $\mathcal{P}_g$ -similarity for the zonal wind (Figure 5). In this situation (Figure 6), a persistent high pressure system is placed in the center of the integration area, blocking the eastward propagation of synoptic disturbances. For example, the low pressure center initially located over Iceland moves northeast-ward and the trough west of Ireland moves towards the British Isles and is dissipated there. In the standard run, this trough is not dissipated as quickly and causes the central European high to be distorted. In the spectral nudging run, on the other hand, the overall evolution is similar to that of the NCEP re-analyses, but the details deviate to some extent.

The different evolutions are revealed by the differences in the air-pressure distributions of the boundary forcing run and the NCEP analyses and of the spectral nudging run and NCEP analysis (Figure 7). Clearly, the air-pressure field in the boundary forcing run deviates on large scales from NCEP. This is particularly striking on 12 March 1993, when over most of the Atlantic negative air pressure deviations prevail. In the spectral nudging run, on the other hand, the differences arise at a smaller spatial scale. Also the magnitude of the differences in the boundary forcing run, reaching values of 15 hPa and higher in all maps of 9-12 March, is considerably larger than in the spectral nudging run, where only a few isolated maxima of about 10 hPa occur.

A comparison with the manually drawn regional analyses of the Berliner Wetterkarte confirms



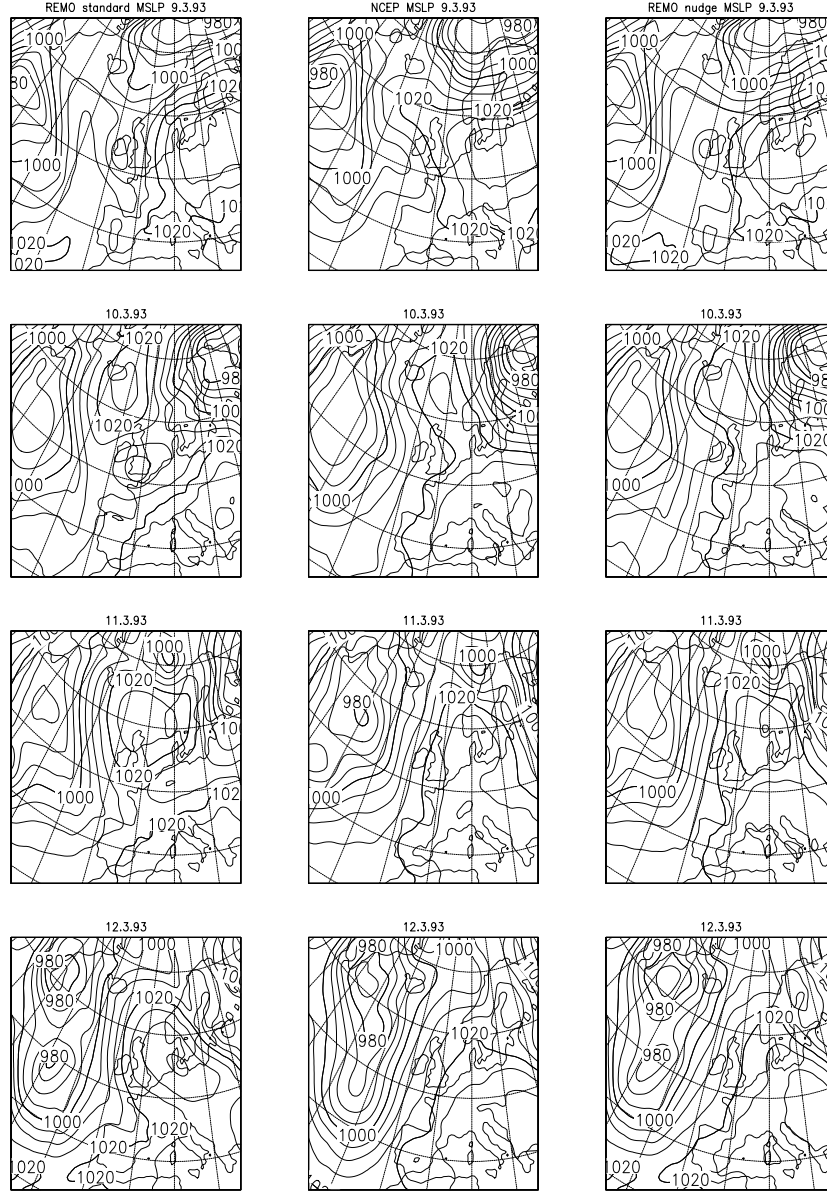


Figure 6: An episode with large differences between the standard run and the spectral nudging run: 9-12 March 1993. Surface air pressure distribution. Left column: boundary forcing run; middle: NCEP analyses (input); right: spectral nudging. Spacing: 5 hPa.

the Berliner Wetterkarte. Also the formation of two separate cyclones over the Atlantic on 12 March is a feature missing in the NCEP re-analyses but identified by the Berlin meteorologists. On the other hand, sometimes NCEP conforms better with the Wetterkarte; for instance on 9

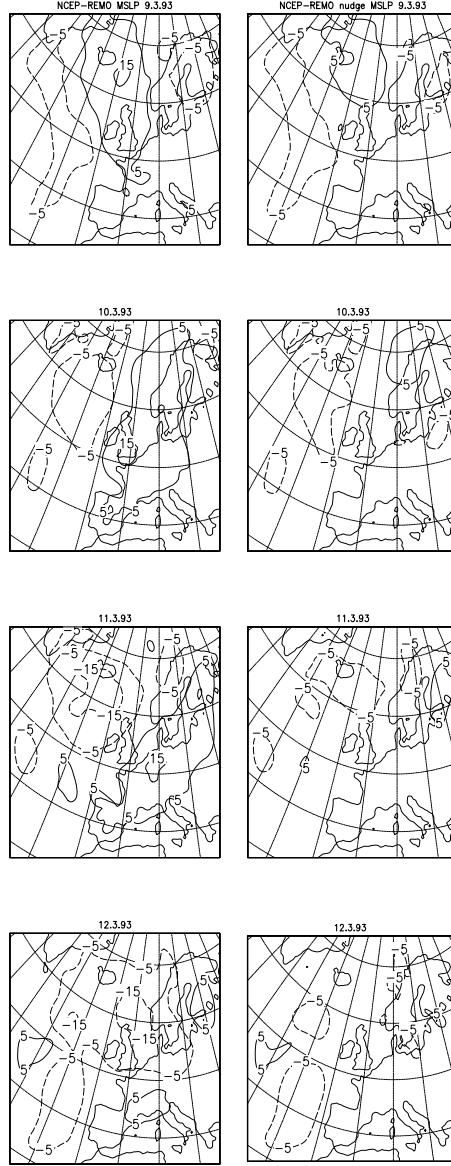


Figure 7: Differences NCEP minus boundary forcing run (left) and minus spectral nudging run (right). Spacing 5 hPa.

March, when the spectral nudging run forms a cut-off low at Ireland, which is merely a trough in NCEP and in the Wetterkarte.

We suggest that the 9-12 March evolution in the standard run takes place because the interior dynamics is not capturing the blocking situation prevailing in the large scale state. Since this

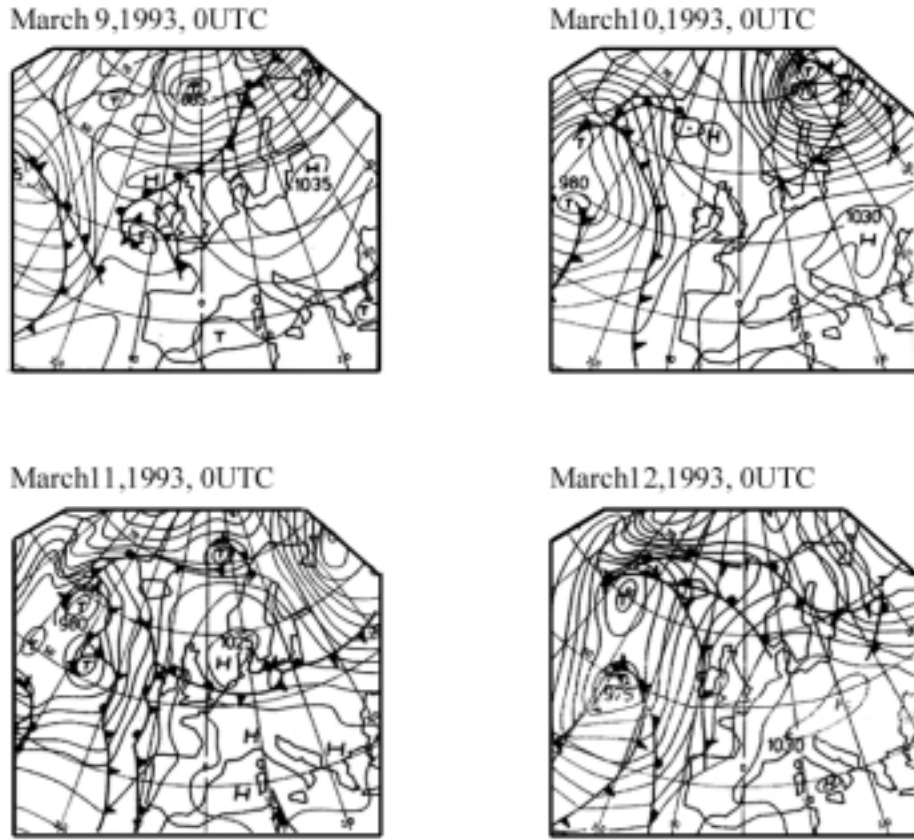


Figure 8: Manual air pressure analyses from Berliner Wetterkarte, 9-12 March 1993.

blocking is hardly encoded in the boundary conditions, the “outer” state given by NCEP and the “inner” state given by the standard REMO run become inconsistent. The spectral nudging technique, however, is efficient enough to keep the “inner” solution on the right trajectory.

Closer inspection of Figure 7 reveals another positive feature of both REMO simulations, namely the small scale features related to fronts which are absent in the NCEP analyses but present in the Wetterkarten of Figure 8. Thus, the spectral nudging does not hamper the emergence of small-scale features.

An intercomparison in the frequency domain reveals that nudging dampens the regional model’s tendency to develop its own low frequency dynamics. Figure 9 shows auto-spectra and squared

coherence spectra for air pressure at the station of de Bilt, The Netherlands, for the driving NCEP analysis (solid) and for the two REMO simulations (dashed). For time periods longer than about 3 days, the REMO standard run generates additional low frequency variance, which is suppressed by the nudging. At higher frequencies, both REMO simulations are rather similar. These findings are supported by the squared coherence spectra between the NCEP analyses and the REMO-simulations; for time periods of 72 hours and more, a much higher coherence is obtained for the spectral nudging run than for the standard boundary control run, whereas for shorter time scales, the coherence drops down and the regional model develops its own dynamics.

## 4.2 Comparison with observational data

The two REMO runs (with standard boundary forcing and spectral nudging) and the NCEP re-analyses (only air pressure and temperature) were compared against observed time series of air pressure, temperature and precipitation at a number of Central European stations. For the time period January - March 1993, also wind observations from the oil field Ekofisk in the Central North Sea were available; these are compared to the REMO simulations as well (the NCEP re-analyses have no surface winds)

For air pressure, REMO returns a bias of about 1 hPa for both formulations whereas NCEP has better mean values (Figure 10). However, the spread of errors is considerably smaller in the case of the spectral nudging simulation.

For the station of De Bilt in the Netherlands, the cumulative distribution functions of the difference in precipitation between the station data, and the two REMO simulations is shown in Figure 11. The large step at zero indicates that, in many cases, both models successfully reproduce dry days. The distributions of positive differences “station minus REMO” are equal in both simulations, but negative differences are strongly reduced for the spectral nudging formulation. For the standard case, the model underestimates the observed precipitation by up to 40 mm/day whereas in the nudging run these deviations are rarely larger than 20 mm/day.

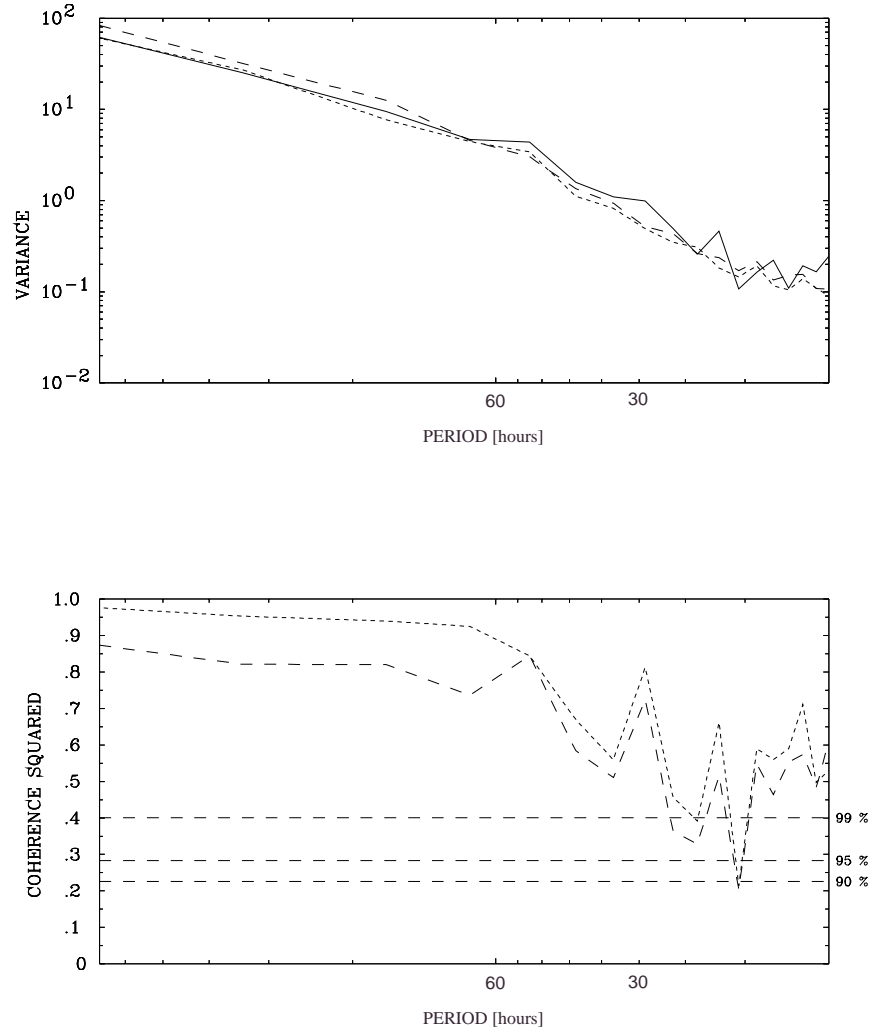


Figure 9: Spectra of analyzed and REMO simulated air pressure at the station De Bilt, The Netherlands.  
Top: Auto-spectra: The solid lines refer to the NCEP analyses, the long dashed line to the standard REMO run, the short dashed line to the spectral nudging REMO run.  
Bottom: Squared coherency spectra; the long dashed line refers to the coherence between the NCEP analyses and the standard run, whereas the shortly dashed line represents the similarity of the spectral nudging run and the analyses.

Figure 12 displays time series of the meridional and zonal components of the wind at 10 m height at Ekofisk in the Central North Sea. Actually, the observations are taken at a higher altitude, and the values are reduced to a standard height of 10 m through a standard calculation.

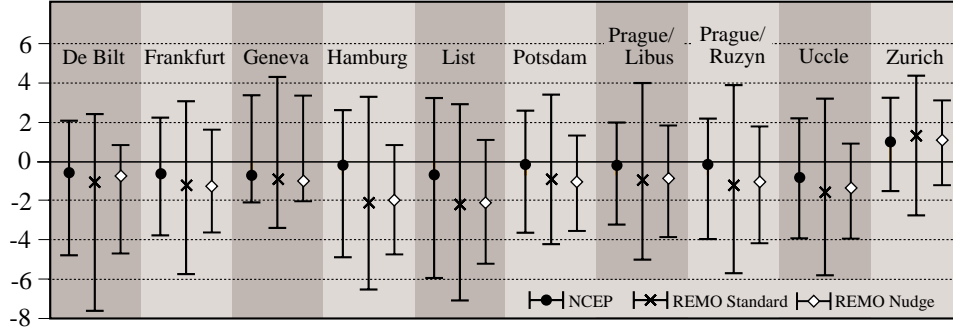


Figure 10: Differences “station data minus simulation” for a series of Central European stations and NCEP, REMO standard and REMO spectral nudging. The variable considered is air pressure. The differences are displayed as mean plus minus one standard deviation.

All three curves coincide relatively well. A remarkable feature is that in many cases the maxima and minima of the wind components of the order of 20 m/s are reproduced. A closer inspection reveals intermittently significant deviations by the standard run and improvements in the spectral nudging run. The 9-12 March episode emerges clearly in the time series of the zonal wind.

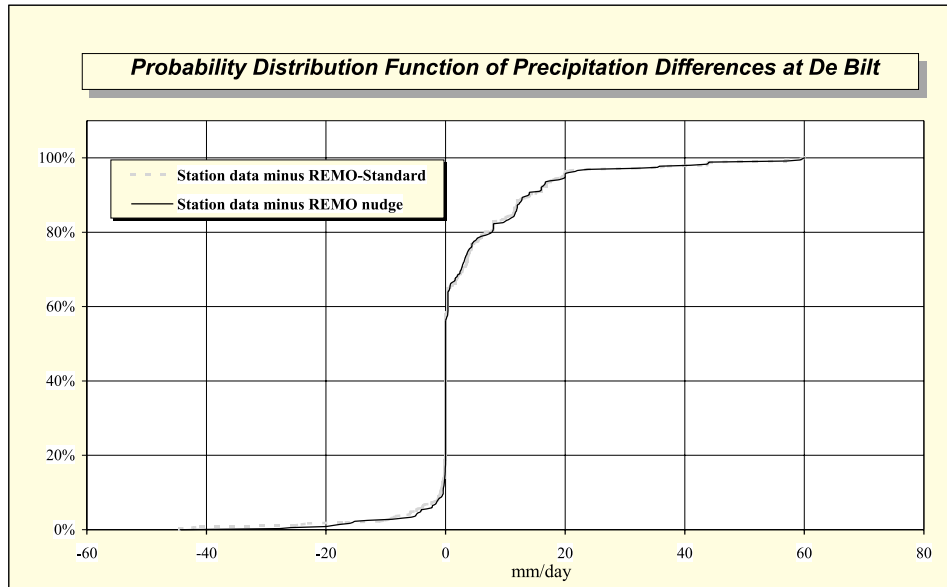


Figure 11: Cumulative distribution function for the difference “de Bilt station data minus simulation” for REMO nudging, REMO standard and NCEP.

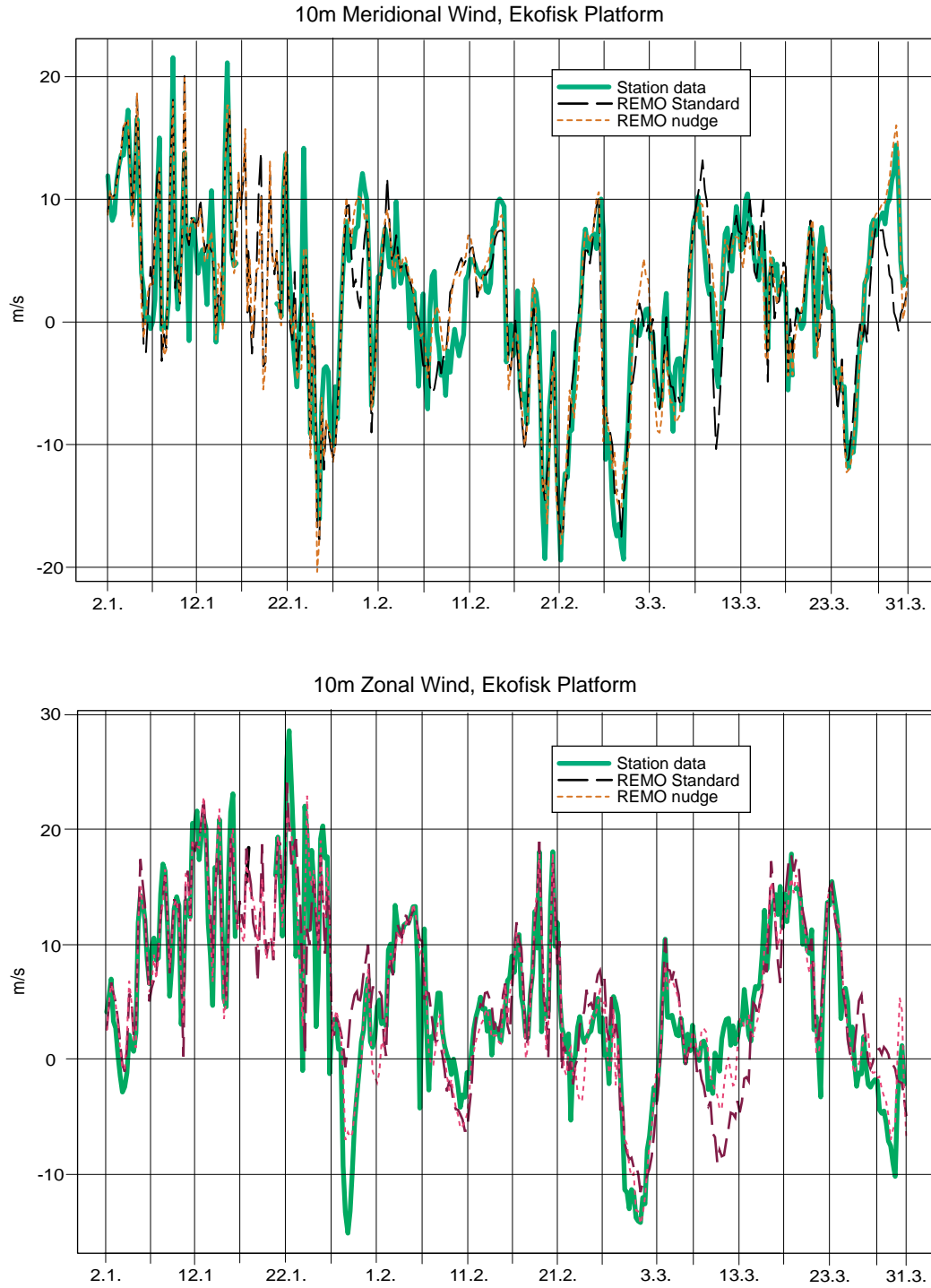


Figure 12: Time series of meridional and zonal wind components at Ekofisk in the Central North Sea from January to March 1993. The observed values are reduced to the standard height of 10m. Broad grey line: observations; light dashed continuous line: REMO spectral nudging, heavy dashed line: REMO standard.

### 4.3 Sensitivity experiments

Two additional simulations have been performed with different values of the nudging coefficient  $\eta^0$ . In one run,  $\eta^0$  was doubled (i.e.,  $\alpha = 0.1$ ), in another simulations halved ( $\alpha = 0.025$ ). In order to save computer time, the sensitivity experiments were done only for one month, starting with state of 1 March of the 3-month spectral nudging run considered so far.

We assess the sensitivity of the simulation to this choice by calculating the measures of similarity  $\mathcal{P}_g$  and  $\mathcal{P}_r$  as defined by (1) for scales well resolved by the NCEP reanalyses and by the REMO simulations only. The time mean measures of similarity, for the zonal and meridional wind components at 500 hPa, is listed in the following table for the different strengths of spectral nudging ( $\alpha > 0$ ) as well as for the standard case ( $\alpha = 0$ ):

Table 2:

	$\mathcal{P}_g$				$\mathcal{P}_r$			
	$\alpha$				$\alpha$			
wind at 500 hPa	0.1	0.05	0.025	0	0.1	0.05	0.025	0
zonal	0.996	0.994	0.991	0.931	0.344	0.325	0.304	0.216
meridional	0.984	0.976	0.964	0.855	0.205	0.239	0.205	0.076

The large-scale control seems to be exerted efficiently also by the other two choices of  $\alpha$ , with markedly higher similarity measures. A more comprehensive study will be needed for designing an optimal configuration of the nudging technique, but this first sensitivity analysis indicates that the performance does not depend significantly on the choice of  $\alpha$ .

## 5 Conclusions

In the present paper we have introduced and tested a new technique to couple a regional climate model to a time variable global or continental state. This concept deviates from the classical approach as the problem is not considered to be a boundary value problem in the grid

point domain, but a downscaling problem. That is, the information which is processed in the model is not so much the state specified at the areal boundaries but at the large-scales. In a generalized sense, this is again a boundary problem, but this time formulated in the spectral domain.

The purpose of the paper was not to delineate the optimal configuration of spectral nudging, but to demonstrate the concept, its feasibility and its potential. Our key argument for the success of the spectral nudging technique is the observations that the nudging technique prevents the regional model to go astray for limited times, generating internal states inconsistent with the driving fields. We have demonstrated that this uncontrolled wandering is not merely a theoretical problem of the regional model forced from the boundaries, but really takes place. At the same time, the spectral nudging forcing does not impede the regional model's ability to develop regional and small scale features superimposed on the large-scale driving conditions.

Different purposes of models require different formulations. When dynamical aspects are to be addressed, such as the dynamics during the genesis of a storm, the spectral nudging should not be used, as it modifies the dynamics inasmuch as it introduces additional forcing terms into the momentum equation. Also, when a significant two-way-coupling is expected to take place, as in the case of the life cycle of a hurricane, the spectral nudging will not be adequate. When, however, specifications of regional climate statistics are needed, such as in paleoclimatic and historic reconstructions and climate change applications, our technique should be preferred as it generates weather streams consistent with the large-scale driving fields.

## 6 Acknowledgments

We are thankful to Daniela Jacob and Ralf Podzun for their help with the model, to Arno Hellbach for helping us accessing the NCEP data, to Lennart Bengtsson for permission to use the model, to Mariza Costa-Cabral and Beate Müller for advice, and to Reiner Schnur for the observational data. Beate Gardeike professionally prepared many of the diagrams. Ralf Weisse made the spectral analysis (Figure 9) for us.

## 7 References

- Davies, H.C., 1976:** A lateral boundary formulation for multi-level prediction models. Quart. J. Roy. Meteor. Soc. 102, 405-418
- G. Doms, W. Edelmann, M. Gertz, T. Hanisch, E. Heise, A. Link, D. Majewski, P. Prohl, B. Ritter and U. Schaettler, 1995:** Dokumentation des EM/DM-Systems. Deutscher Wetterdienst Abteilung Forschung, Offenbach a.M.
- Frey-Buness, F., D. Heimann and R. Sausen, 1995:** A statistical-dynamical downscaling procedure for global climate simulations. Theor. Appl. Climatol. 50, 117-131
- Friedman, R.M., 1989:** Appropriating the Weather. Vilhelm Bjerknes and the construction of a modern meteorology. Cornell University Press, 251 p, ISBN 0 8014-2062-8
- Fuentes, U. and D. Heimann, 1996:** Verification of statistical-dynamical downscaling in the Alpine region. Clim. Res. 7:151-186
- Giorgi F., 1990:** Simulations of regional climate using limited-models nested in a general circulation model. J. Climate 3, 941-963
- Giorgi, F., M.R. Marinucci and G.T. Bates, 1993:** Development of second-generation regional climate model (RegCM2). Part II: Convective processes and assimilation of lateral boundary conditions. Mon. Wea. Rev. 121, 2814-2832
- Jacob, D., and R. Podzun, 1997:** Sensitivity studies with the regional climate model REMO. Meteorol. Atmos. Phys. 63, 119-129
- Jacob, D., R. Podzun and M. Claussen, 1995:** REMO - A model for climate research and weather prediction. International Workshop on Limited-Area and Variable Resolution Models, Beijing, China, October 23-27, 1995, 273-278
- Kalnay, E., M. Kanamitsu, R. Kistler, W. Collins, D. Deaven, L. Gandin, M. Iredell, S. Saha, G. White, J. Woollen, Y. Zhu, M. Chelliah, W. Ebisuzaki, W. Higgins, J. Janowiak, K.C. Mo, C. Ropelewski, J. Wang, A. Leetmaa, R. Reynolds, R. Jenne, and D. Joseph, 1996:** The NCEP/NCAR 40-Year Reanalysis Project. Bull. Amer. Meteor. Soc. 77, 437-471
- Kauker, F., 1998:** Regionalization of climate model results for the North Sea. PhD thesis

University of Hamburg, 109 pp.

**Kida, H., T. Koide, H. Sasaki and M. Chiba, 1991:** A new approach to coupling a limited area model with a GCM for regional climate simulation. J. Meteor. Soc. Japan 69, 723-728

**Kidson, J.W. and C.S. Thompson, 1998:** Comparison of statistical and model-based downscaling techniques for estimating local climate variations. J. Climate 11, 735-753

**Sasaki, H., J. Kida, T. Koide, and M. Chiba, 1995:** The performance of long term integrations of a limited area model with the spectral boundary coupling method. J. Meteor. Soc. Japan 73, 165-181

**von Storch, H., 1995:** Inconsistencies at the interface of climate impact studies and global climate research. Meteorol. Z. 4 NF, 72-80

**von Storch, H., 1999:** The global and regional climate system. In: H. von Storch and G. Flöser (eds): *Anthropogenic Climate Change*, Springer Verlag, ISBN 3-540-65033-4, 3-36